Adsorption and Coadsorption of CO and H on Ruthenium Surfaces

I. M. Ciobica,*,†,‡ A. W. Kleyn,‡,§ and R. A. Van Santen†

Schuit Institute of Catalysis, Eindhoven University of Technology, P.O. Box 513, 5600 MB Eindhoven, The Netherlands, FOM-Institute for Atomic and Molecular Physics, Kruislaan 407, 1098 SJ Amsterdam, The Netherlands, and Leiden Institute of Chemistry, P.O. Box 9502, 2300 RA Leiden, The Netherlands

Received: January 17, 2002

The interaction of CO with the Ru(0001) surface at several coverages (11.1, 25.0, and 33.3%) is studied, as well as the interaction of CO with a stepped Ru(0001) surface. The preference for the adsorption site (atop versus hcp) is analyzed with density of states diagrams. Hydrogen layers can be densely packed; 1 ML could, in fact, correspond to more than 100% coverage, where 100% coverage would correspond to one addatom for each metal atom on the surface. Calculations are made for 1 ML of adsorbed hydrogen up to 300% coverage for 2×2 supercells. The H coadsorption with CO (2×2 (CO + *n*H), $n = 1, 3, 4$) is discussed for different adsorption sites. The lateral interaction H−CO is repulsive. H_{ads} and CO_{ads} prefer to form islands rather than mixed structures. CO is little influenced by coadsorption, except when 1 ML of atomic hydrogen is preadsorbed. H is strongly affected by coadsorption. The H adsorption sites become highly asymmetrical if H and CO share one metal atom.

1. Introduction

The adsorption of CO to metal surfaces has over the years become the prototype system for molecular chemisorption. A rather simple bonding model has in general been accepted. It is known that on the late transition metals the energetic difference between free and adsorbed CO (the heat of adsorption) is much smaller than the C−O dissociation energy (1084 kJ mol^{-1} or 11.23 eV).[1] The adsorption of carbon monoxide and the coadsorption with hydrogen on the close-packed Ru(0001) surface is particularly interesting because of its relevance to the Fischer−Tropsch synthesis and the methanation reaction.[2] Whereas both CO and H_2 adsorption on the ruthenium surface has been studied quite extensively over the past decades, very little information is available for the hydrogen−carbon monoxide coadsorption system on Ru(0001).

The saturation fractional coverage of dissociatively chemisorbed molecular hydrogen is one adatom per Ru(0001) unit cell.[3] Whereas at low surface coverages hydrogen resides in the fcc 3-fold hollow sites, at saturation coverage, hydrogen was found to occupy a site of slightly reduced symmetry. This is presumably due to either a shift of the hydrogen adatom toward the bridge position or a reconstruction of the ruthenium surface.[4]

The CO on the Ru(0001) adsorption system has been widely studied.[5,6] CO is known to adsorb nondissociatively[5] in the upright position with the C-end facing the surface.[7] Adsorption is nonactivated, and a precursor model including two intrinsic and one extrinsic precursor has been proposed[8] for a surface partially covered by CO. The adsorption energy varies with coverage from 160 to 175 kJ mol^{-1} [9,10] in the 0.33- to 0-ML coverage regime. The preferred site is the atop site for coverages up to 0.33 ML.[6]

Molecular-beam scattering experiments of NO or CO at Ru(0001)−H(1×1) yielded some quite remarkable observations. At first, the angular distributions of the scattered CO and NO in the energy region of thermal to 250 kJ mol^{-1} are remarkably sharp. In fact, these are the sharpest angular distributions ever measured for molecular scattering at surfaces.[11−16] This strongly suggestes that the hydrogen completely eliminates the binding potential of the Ru(0001) surface, turning it into a flat molecular mirror. However, measurements of the sticking coefficient do not confirm this. The sticking coefficient is nonzero for energies above 20 kJ $mo1^{-1}$ and increases to values exceeding 0.1.[11−13] This suggestes that the unit cell can be divided into three regions: a reflection region, a sticking region, and a transition region in between.[14] The presence of the coexistence of a chemisorbed CO species with a compressed and presumably quite flat H-region was confirmed by our first calculations on this system.[13] The calculations indicated that CO adsorbed on Ru(0001)−H(1×1) is much less strongly bound than CO and H on the bare surface and that phase separation is likely, as has been observed.[17,18]

CO adsorption and dissociation on transition metals has also been investigated quite extensively on a theoretical basis by applying various computational methods. Delbecq et al. investigated CO and NO adsorption on Pd(100), Pd(111), Pd_3Mn(100), and Pd_3Mn(111) using extended Hückel[19] and DFT[20,21] methods. The bridge and the 3-fold hollow sites are preferred for the CO adsorption on bare Pd surfaces. On the alloy surfaces, CO adsorption is weaker.

LDA calculations were carried out by Eichler et al.[22] to examine the CO adsorption behavior on the Rh(100) surface. The bridge position is the most stable adsorption site for CO at all coverages. The ratio between CO molecules adsorbed on the bridge and CO adsorbed atop is not constant with the coverage. The difference between the adsorption energies for bridge and atop position shows a minimum at half-coverage. At high coverage, CO forms a pseudohexagonal overlayer with p4($\sqrt{2} \times \sqrt{2}$) periodicity.

Large-scale DFT calculations were used by Hammer et al. to investigate the interaction of CO with stepped and reconstructed Pt surfaces.[23] The adsorption energy on the steps is 70

* Corresponding author. E-mail: i.m.ciobica@TUe.nl.
† Eindhoven University of Technology.
‡ FOM-Institute for Atomic and Molecular Physics.
§ Leiden Institute of Chemistry.

10.1021/jp0201478 CCC: $25.00
Published on Web 12/05/2002

kJ mol^{-1} higher than on the flat terraces. The differences become larger, up to 100 kJ mol^{-1}, if the adsorption energies on kinks are compared.

A systematic study of the adsorption of CO on Pt(100), Pt(110), and Pt(111) is presented by Curulla et al. using HF ab initio cluster models.[24] The geometries and vibrational frequencies are invariant with the cluster size; however, the adsorption energies are very sensitive to the cluster size. The bonding interaction is dominated by the π back-donation, although the σ donation plays a significant role.

A database of DFT GGA calculations of the chemisorption energies of CO over hexagonal compact surfaces of Ni, Cu, Ru, Pd, Ag, Pt, Au, and Cu_3Pt is provided by Hammer et al.[25] The smallest adsorption energy is for Au(111) and Ag(111) whereas Ru(0001) gives the highest adsorption energy from this series.

Wang et al. reported a study of CO coadsorption with atomic O on Ru(0001) focusing on the tilting of CO.[26] The DFT calculations have been performed with a cluster model. The interaction between CO and O can be described as field-induced chemistry: the charged atomic oxygen creates a local electrostatic field along the CO adsorption site that modifies the metal−carbon and the C−O bonds, resulting in a tilt of the molecule. Peebles et al.[27] showed experimentally that the CO sticking probability drops with increasing deuterium coverage, meaning that deuterium acts as a site blocker for CO adsorption. There was no evidence of a chemical reaction between hydrogen and CO at 100 K, and no additional thermal desorption states appear in the TPD. A strong repulsive interaction between the deuterium atoms and carbon monoxide was also found. Further evidence for this observation was provided by Mak et al.,[28] who determined the hydrogen diffusion coefficients as a function of preadsorbed CO coverage ($\theta_{CO} = 0-0.2$ ML) at $T = 260$ K with LITD. They found a hydrogen-exclusion radius that is on the order of the van der Waals radius of the CO molecule. However, even on a fully deuterium-saturated surface, considerable amounts of CO, up to 20% of the CO saturation coverage, could be adsorbed.[27] Since the D−CO interaction is repulsive in the mixed overlayer and deuterium blocks adsorption sites, an interesting question is how a gas-phase CO molecule adsorbs in the hydrogen overlayer.

The coadsorption of CO and hydrogen on several transitional metal surfaces has been reviewed by White et al.[17] with the conclusion that CO and hydrogen form segregated rather than mixed structures on the close-packed (fcc(111), hcp(0001)) surfaces. This is attributed to a strong repulsive H−CO interaction on the surface, which is the dominant lateral interaction in these coadsorbed systems.

In the current study, DFT calculations have been carried out to provide better insight into the dynamic process of the coadsorption of CO and H as well as of the separated adsorptions.

2. Method and Surface Model

The quantum chemical studies were performed using the VASP[29,30] code, which allows periodic DFT calculations with pseudopotentials and a plane wave basis set. The approach implemented in the program is based on a generalized gradient approximation with the Perdew−Wang 91 functional.[31] When Methfessel and Paxton's smearing method[32] ($\sigma = 0.2$ eV) is applied to the electron distribution, the free energy is the variational quantity, and the energy is extrapolated for $\sigma = 0.0$. The interactions between the ions and the electrons are described by ultrasoft pseudopotentials (US-PP) introduced by Vanderbilt[33] and provided by Kresse and Hafner.[34]

TABLE 1: Adsorption Energies for CO on Ruthenium Surfaces, Different Sites, and Different Coverages

coverage (%)	structure	adsorption site	adsorption energy (kJ × mol^{-1})
25.0	2 × 2	atop	−177
25.0	2 × 2	hcp	−176
25.0	2 × 2	fcc	−169
25.0	2 × 2	bridge	−160
25.0	2 × 2	atop tilted versus fcc	−177
25.0	2 × 2	atop tilted versus hcp	−183
25.0	2 × 2	hcp tilted	−176
25.0	2 × 2	fcc tilted	−
25.0	2 × 2	bridge tilted	−167
33.3	$\sqrt{3} \times \sqrt{3}$	atop	−189
33.3	$\sqrt{3} \times \sqrt{3}$	hcp	−177
33.3	$\sqrt{3} \times \sqrt{3}$	fcc	−170
33.3	3 × 3	bridge	−166
11.1	3 × 3	atop	−186
11.1	3 × 3	hcp	−186
	steps	atop edge	−195
	steps	hcp edge	−195
	steps	hcp bottom	−180

We used a four-layer slab with five vacuum layers in between in a 2 × 2 supercell to describe the surface. The structures where the second layer of H atoms was formed were also calculated with seven vacuum layers, but the differences were less than 0.5 kJ mol^{-1}. Adsorption on both sides with an inversion center prevents the generation of dipole−dipole interactions between the supercells. The k-points sampling was generated by following the Monkhorst−Pack procedure with a 5 × 5 × 1 mesh. The 3 × 3 supercell was also a four-layer slab with five vacuum layers in between the slabs. The k-points sampling used a 3 × 3 × 1 mesh.

To model the steps, we consider a cell with double steps, where the number of atoms in each (0001) terrace is two and three, respectively.

The cutoff energy for the plane waves basis set is 400.0 eV in the case of CO adsorption and H coadsorption and 300.0 eV in the case of H adsorption. The coordinates of all atoms were fully optimized. All of the parameters (the k-points mesh, the number of metal and vacuum layers, etc.) were tested and carefully selected.[35]

3. Results and Discussion

Initially, we will discuss the site preference of CO on different ruthenium surfaces. On some metals, the atop site is preferred, whereas on others, the hollow site is preferred. Ruthenium is a case for which both sites show similar adsorption energies. In the second part, we we show results for the calculations of a compressed monolayer of H atoms on the Ru(0001) surface. The calculations are performed for a coverage of 25 to 300%. In the third part, we show how lateral interactions affect the coadsorbed H atom with CO.

3.1. Adsorption of Carbon Monoxide on the Flat and Stepped Ru Surfaces. The molecular adsorption of CO on the ruthenium surfaces is nonactivated. On the Ru(0001) surface, for the 2 × 2 structure (25% coverage), our calculations give an adsorption energy of −177 kJ mol^{-1} for the atop site and −176 kJ mol^{-1} for the hcp hollow site. This agrees well with experimental results.[10] The fcc hollow site gives an adsorption energy of −169 kJ mol^{-1}, and the bridge site, −160 kJ mol^{-1}; see Table 1. Since all of those adsorption energies are very close, the CO molecule is very mobile, and CO diffusion is not activated.

Other 2 × 2 calculations were performed for a CO molecule adsorbed in a tilted geometry. The adsorption energy did not

change significantly. For the atop site, the CO molecule was tilted in the direction of a nearby hcp site or a nearby fcc site; the adsorption energies are −177 and −183 kJ mol^{-1}, respectively (0 and 6 kJ mol^{-1}, respectively, more stable than the nontilted ones) for angles of 0.5° and 1.6°, respectively. CO tilted on the hcp site is not stable; the final tilting angle is 0°. By tilting the CO from an fcc site, the molecule is migrating to the nearby atop site. The tilted CO on a bridge site gives an adsorption energy of −167 kJ mol^{-1} (6 kJ mol^{-1} more stable than the nontilted one), and the tilting angle is 9.0°.

A few calculations for CO adsorption with the O-end pointing toward the surface were performed for the fcc and hcp sites. The CO−surface interaction is repulsive; by fixing the molecule in this position, the adsorption is around +100 kJ mol^{-1} (less stable than separately), and if the separation is allowed, the CO molecule will go as far it can go (to the top of the cell) and the adsorption energy is going to zero.

The parallel adsorption mode was also investigated. The CO molecule is not stable parallel with the surface. The final adsorption mode is then the CO molecule with the C-end pointing toward the surface, as proposed by Fuggle and others.[5−7] A similar orientational dependency has been proposed for NO on Pt(111) by Lahaye et al.[36]

To fully understand the adsorption of CO on this surface, we also performed calculations for CO adsorption for the $\sqrt{3} \times \sqrt{3}$ R30° structure (33.3% coverage). In this case, the atop site becomes more stable. The adsorption energy is −189 kJ mol^{-1} whereas for the hollow hcp site it remains −177 kJ mol^{-1}. The other 3-fold site (fcc) has an adsorption energy for CO of −170 kJ mol^{-1} and the bridge site, −166 kJ × mol^{-1}; see Table 1.

The fragile balance for atop/hcp adsorption of CO on Ru(0001) is in favor of the atop site for the $\sqrt{3} \times \sqrt{3}$ structure (33.3% coverage). For the 2 × 2 structure (25.0% coverage), both sites have the same stability. It seems that the lateral interaction of CO atop is more important that the interaction of CO hcp since the adsorption energy does not change with the coverage for the hcp site but it changes for the atop site.

Calculations for the 3 × 3 structure (11.1% coverage) for CO adsorption atop and on hcp sites were performed as well. The adsorption energy is −186 kJ mol^{-1} for the atop site and for the hcp site.

The C−O bond length is 1.17 Å for the atop site, 1.18 Å for the bridge site, and 1.19 Å for the 3-fold hollow sites (hcp and fcc) for 2 × 2, $\sqrt{3} \times \sqrt{3}$, and 3 × 3 structures, tilted or not. The Ru−C bonds are 1.90 Å for the atop absorptions, 2.05−2.11 Å for the bridge sites, and 2.09−2.15 Å for the 3-fold hollow sites. The C−O bond length and the Ru−C bond length are getting slightly longer for more metal atoms around the C atom. The Ru−C−O angle varies between 178 and 180° for the atop adsorption mode, 134−142° for the bridge, and 131−136° for the 3-fold hollow sites. The Ru−C−Ru angles are between 81 and 82° for bridge sites and between 76 and 80° for 3-fold hollow sites.

Steps were also considered. Since Ru is an hcp metal, the steps presented on the Ru(0001) surface are not the same, but two different ones are repeated regularly. The adsorption energy of the CO atop edge of one such step is −195 kJ mol^{-1}. The adsorption energy of the CO hcp at the edge of the step is −195 kJ mol^{-1} whereas at the bottom of the same step it is −180 kJ mol^{-1}; see Figure 1. If two CO are adsorbed in the hcp site at the step edge and in the hcp site at the step bottom, then the adsorption energy is −161 kJ mol^{-1} for each CO molecule.

The geometry of the CO adsorbed atop on the step edge is not different from the other CO adsorbed atop on plain surfaces, except that the CO molecule is tilted more—the angle with the (0001) surface is 5°. The geometry of the CO adsorbed hcp on the step edge and the bottom edge is different from that of the adsorbed CO on the plain surface. The C−O bond lengths are 1.20 and 1.30 Å, respectively. The CO adsorbed on the hcp edge has two short C−Ru bonds of 2.08 Å and a long C−Ru bond of 2.36 Å whereas the other CO molecules have three bonds of 2.08 Å. The angles O−C−Ru are 124 and 2 × 137° for edge hcp and 156 and 2 × 118° for bottom hcp. The Ru−C−Ru angles are 74, 74, and 83° and 82, 79, and 79°, respectively. The O from the adsorbed CO on the bottom hcp is close to the two metal atoms from the step edge; the O−Ru distance is 2.32 Å. When two CO molecules are adsorbed, one on the edge hcp and one on the bottom hcp, the one that is edge hcp is less perturbed, the same C−O and C−Ru are present, and the angles O−C−Ru and Ru−C−Ru are similar within a few degrees. The other CO, adsorbed on bottom hcp, is more affected. The C−O bond length is a bit shorter (1.26 Å) and the C−Ru bonds are different (2.03, 2.15, 2.15 Å), but the angles O−C−Ru and Ru−C−Ru are the same. The O−Ru from the edge is a bit longer (2.52 Å).

Vibrational frequencies were computed with the AnharmND[37] program for CO in the gas phase and CO adsorbed on atop and hcp sites in 2 × 2 structures. In Table 2 , you can see the results. Three points were calculated for each side of the parabola, and the results were interpolated to calculate the harmonic and anharmonic frequencies. Experimental values are taken from ref 38.

We analyzed the local density of states (LDOS) for the CO molecules adsorbed on atop and hcp sites for 2 × 2, 3 × 3, and steps. See Figures 2 and 3 for the DOS diagrams for the p_x and p_z orbitals of the C atom from the CO molecule.

Considering the CO adsorbed atop, for the p_x orbital, we can see that the $2\pi^*$ is broader and a very small amount is filled (under the Fermi level). There is a small difference between the CO adsorbed in 2 × 2 and 3 × 3 as well as the CO atop on the step edge.

For the p_z orbital, we can see that the 5σ is similar for the three cases. A common feature for CO adsorbed atop would be that on the step edge, the broadening of the antibonding orbitals is smaller.

Considering the CO adsorbed in the hcp 3-fold hollow site, for the p_x orbital, we can see that the $2\pi^*$ is also broadened. Compared with the atop adsorption, the $2\pi^*$ is just a little bit higher in energy for the hcp adsorption.

For the p_z orbital, we can see that the 5σ is split in the case of CO at the step bottom because of the interaction with more than three metal atoms. Compared with the atop adsorption, the 4σ and 5σ are at the same level, but somehow the 3σ is higher in energy for the hcp adsorption. This could explain the (small) difference in the adsorption energy for atop and hcp adsorption sites.

3.2. High-Coverage Hydrogen on the Ru(0001) Surface. Because the H atom is small, the compression of the adsorbed layer has to be easier than with any other atom. In this study, we will show that, if at lower coverage the adsorption sites are well defined, then at higher coverage the H atoms are sitting on the surface in no particular site.

We calculate the adsorption of H atoms in 2 × 2 unit cells for 25−300% coverage in 10 cases each for several different structures. The energies of those structures can be seen in Figure 4.

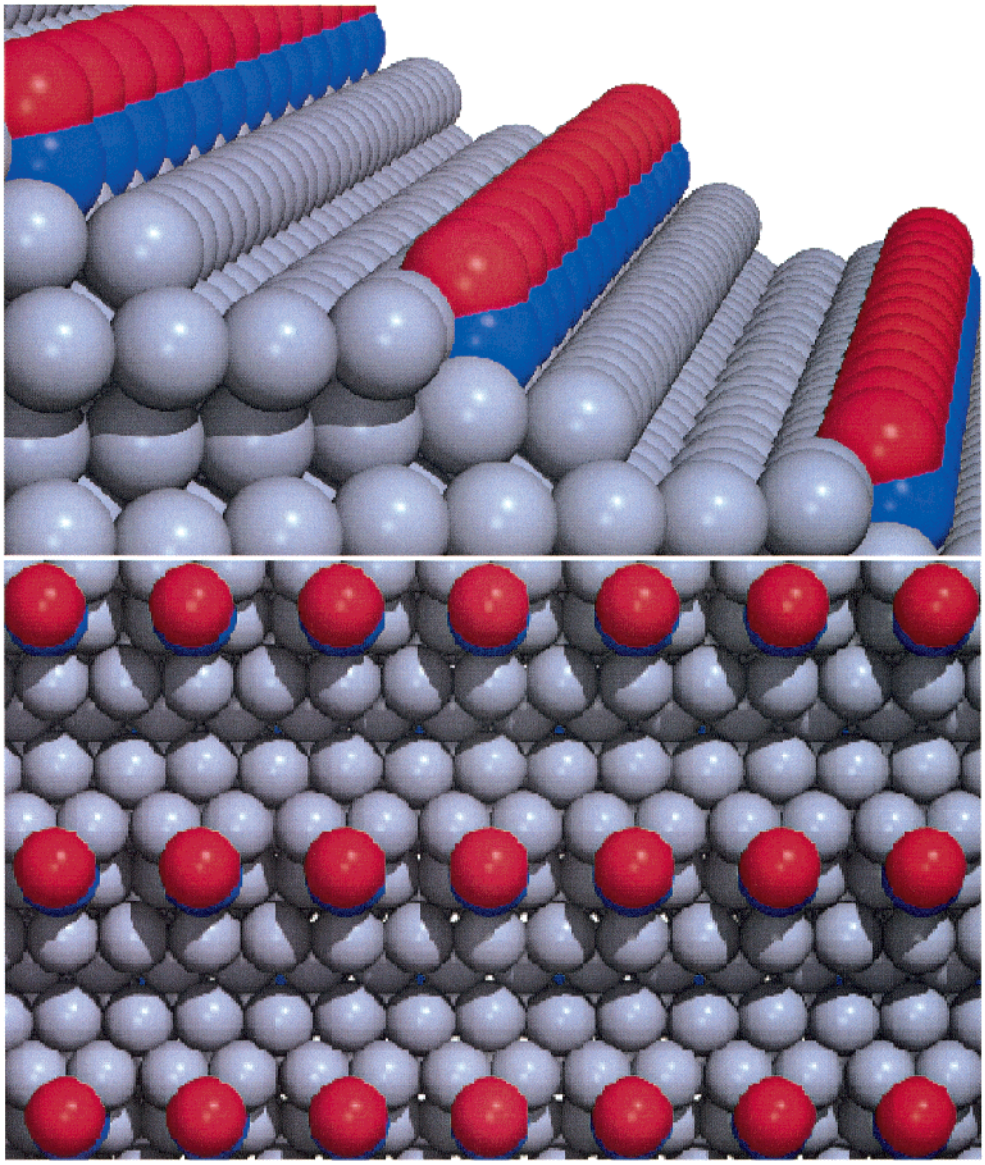

Figure 1. CO adsorbed on the bottom of the steps. Top and side views.

TABLE 2: Frequences for CO in the Gas Phase and Adsorbed on Ru(0001) Atop and on the Three-Fold hcp Hollow Site

	frequences in cm^{-1}		
adsorption site	harmonic	anharmonic	experimental
gas phase	2134	2103	2170
atop	1964	1940	1989[38]
			1990[40]
hcp	1765	1727	unknown

For 25% coverage, we calculate the adsorption of H in fcc and hcp 3-fold hollow sites as well as at atop and bridge sites. The H subsurface is unstable at this coverage (in the octahedral site as well as in the two tetrahedral sites). The fcc site gives an adsorption energy of -53 kJ mol^{-1} whereas the hcp site gives 50 kJ mol^{-1}. The bridge site is less stable, with an adsorption energy of -41 kJ mol^{-1}, and the atop site is the most unstable, with an adsorption energy of -9 kJ mol^{-1}. See in Table 3 how this will change later on.

For 50, 75, and 100% coverages, the adsorption of two, three, or four H atoms in the 2×2 unit cell did not change the adsorption energies for the fcc and hcp sites too much. The lateral interaction at this coverage is still low. For the mixed cases, H fcc and H hcp, when the H atoms share one metal atom (are "far" apart), the adsorption energy is still not affected, and when they share two metal atoms (are "close"), the adsorption energydecreases.

The geometries of H atoms adsorbed on the Ru(0001) surface change little up to 100% coverage, except for the close adsorption case. The usual Ru−H bond lengths are between 1.85 and 1.90 Å for H atoms adsorbed in hollow sites (fcc and hcp). If two H atoms share two metal atoms on the surface, they will be displaced from the center or the hollow site, and the three bonds with the metal will be one shorter, around 1.70−1.76 Å, and two longer, around 1.95−2.05 Å. For the bridge site, the adsorbed H atom will have Ru−H bonds lengths of 1.75−1.80 Å whereas the atop site will have Ru−H distances of around 1.60 Å.

In Figure 5, you can see the difference between a far adsorption or a close adsorption of two H atoms. For the far adsorption, the H atoms share one metal atom on the surface. The geometries are not affected. For the close adsorption, the H atoms share two metal atoms on the surface. The geometries are affected. The H fcc have a shorter Ru−H distance of 1.81 Å and two long ones of 1.96 Å. The H hcp will have a short distance 1.73 Å and two long ones of 1.98 Å.

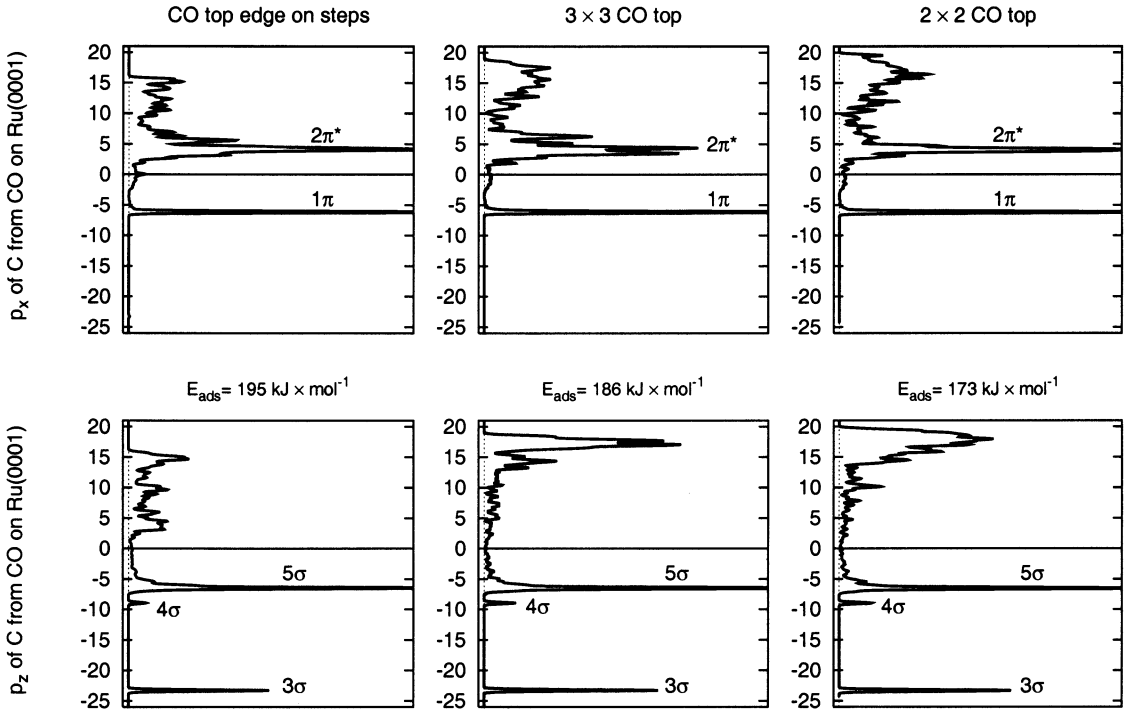

Figure 2. DOS diagrams for p_x and p_z orbitals of the C atom from the CO molecule's adsorbed atop sites.

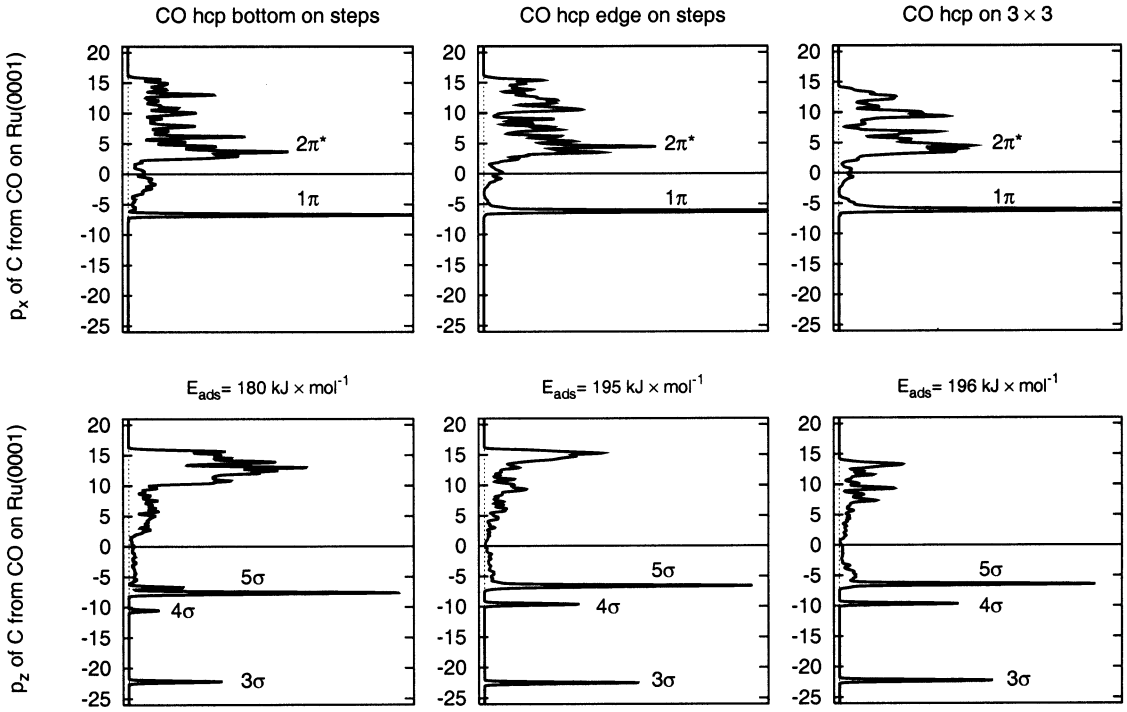

Figure 3. DOS diagrams for p_x and p_z orbitals of the C atom from the CO molecule's adsorbed hcp sites.

At 100% coverage, the mixed adsorption of H is shown in Figure 6. The "Y"-like structure formed by an atom in a hollow site and three others in the other kind of hollow site is a structure that we will also see at higher coverages. The H adsorbed in the middle is still symmetric, with a Ru−H bond of 1.85 Å. The other three atoms are perturbed, with a short bond around 1.72−1.75 Å and two long ones around 2.03−2.04 Å.

Going over the classical 1 ML, for 125% coverage, we have to accommodate five H atoms in the same unit cell. Jachimowski et al.[39] have shown that 1 ML of H on Ru(0001) can contain up to 142% coverage. Several possible structures are shown in Figure 7. (a) and (b) are similar to the previous Y-like structure with an extra atom adsorbed in a nearby empty site. (c) and (d) look similar with 4H fcc and 4H hcp, respectively, where one H atom is replaced with a pair of H atoms in bridge sites competing for the same hollow site. The H atoms from hollow sites are little affected, with two normal Ru−H bonds and a slightly longer one (1.94−2.07 Å). The H atoms from the bridge sites also have normal bonds (for a bridge site) of 1.78 Å. The $H_{bridge}-H_{bridge}$ separation is 1.75 Å.

At 150% coverage, the bridge site becomes the most populated site. Six H atoms can sit in the same unit cell. The

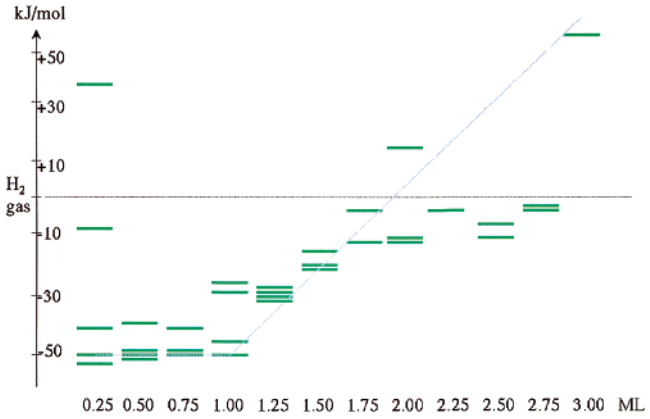

Figure 4. Energy diagram (in kJ mol^{-1} per H atom relative to $^1/_2H_2$ in the gas phase) for H adsorption on Ru(0001) at several coverages (1 ML = 100% coverage = 4H atoms per 2 × 2 unit cell).

configuration with the 2H fcc + 2H hcp + 2H bridge is derived from two situations: 4H fcc + 2H hcp and 2H fcc + 4H hcp, where two H fcc (hcp) are going to be a bridge in an end-symmetric situation. For this coverage, the adsorbed H is still more stable than the gas-phase one.

In Figure 8 , four structures for H adsorption at 150% coverage are presented. In (a), the H in fcc and the one in hcp have similar bond lengths of 1.80 Å and two of 1.90 Å. The H atoms in bridge sites have two bonds between 1.78 and 1.80 Å. In (b), the H atoms in the hollow sites have a short bond of 1.75−1.77 Å and two long ones of 1.94 Å. The (c) structure is highly asymmetric. All H atoms in hollow sites have a short and two long Ru−H bonds; the H atoms in bridge sites also are slightly distorted. The H atoms atop have bonds of 1.61 Å. The (d) structure is more symmetric, with three H atoms competing for the same fcc site and three H atoms competing for the same hcp site. Their H−Ru distances are 1.78−1.80 Å. This situation, of three H bridge atoms around a hollow site (like a "Δ"), is to be seen also at higher coverage.

At 175% coverage, seven H atoms can be accommodated on the unit cell. Two structures are presented in Figure 9. (a) is composed of a Y structure and a Δ. A similar structure (not shown) is obtained simply by replacing the fcc site with the hcp one. For the (b) structure, the H atoms in hollow sites have two short bonds of 1.77−1.82 Å and a long bond of 2.06−2.10 Å. The H atoms adsorbed in bridge sites have bonds of 1.74−1.81 Å, and the H atoms in atop sites have Ru−H bond lengths of 1.62 Å. The $H_{fcc}-H_{atop}$ and $H_{atop}-H_{bridge}$ separations are between 1.56 and 1.62 Å. At 200% coverage, eight atoms have to stay in the same unit cell. 4H fcc + 4H hcp is less stable than the H_2 in the gas phase with 11 kJ mol^{-1}, but if 4H are going atop, then we have a stable situation: 4H fcc + 4H atop (−13 kJ mol^{-1}) or 4H hcp + 4H atop (−14 kJ mol^{-1}).

At 250% coverage, the adsorption energies would change the sign, so the monolayer picture would start to collapse. H_2 molecules start to form in the second monolayer, or H_2 molecules standing with only one H interacting with the surfaces or the subsurface H (in the octahedral site) or a mixture of those situations, in order to lower the energy.

In Figure 10 , one can see two structures such as that (a) consists of four H atoms in fcc sites, one H atom in an octahedral subsurface site, three H atoms atop, and above the other atop site is the H_2 molecule. The subsurface H atom has bonds of 1.97 Å with the Ru atom from the first layer and 1.92 Å with the Ru atoms from the second layer. The H−H bond length in the H_2 molecule is 0.75 Å. The separations between the Ru atom and each of the two H atoms from H_2 are 3.70 and 4.19 Å, the H_2 molecule being tilted. (b) consists of fewer atoms in the first layer and two H_2 molecules on the second layer. The H adsorbed in the fcc site is slightly disturbed; the other H atoms have typical bond lengths. The H−H bonds in H_2 are 0.75 Å,

TABLE 3: Adsorption Energies for H on Ru(0001) at Different Coverages[a]

coverage (%)[b]	sites f	h	b	t	s	p	adsorption energy (kJ × mol^{-1})	obsd
25	1	0	0	0	0	0	−53	
	0	1	0	0	0	0	−50	
	0	0	1	0	0	0	−41	
	0	0	0	1	0	0	−9	
	0	0	0	0	1	0	+37	octahedral site
	0	0	0	0	1	0	+60	tetrahedral site 1−3
	0	0	0	0	1	0	+96	tetrahedral site 3−1
50	2	0	0	0	0	0	−51	
	0	2	0	0	0	0	−48	
	1	1	0	0	0	0	−52	far
	1	1	0	0	0	0	−39	close
75	3	0	0	0	0	0	−51	
	0	3	0	0	0	0	−48	
	2	1	0	0	0	0	−42	
	1	2	0	0	0	0	−42	
100	4	0	0	0	0	0	−51	
	0	4	0	0	0	0	−47	
	3	1	0	0	0	0	−29	
	1	3	0	0	0	0	−26	
125	4	1	0	0	0	0	−31	
	1	4	0	0	0	0	−29	
	3	0	2	0	0	0	−30	
	0	2	3	0	0	0	−28	
150	2	2	2	0	0	0	−21	
	1	1	4	0	0	0	−15	
	2	1	2	1	0	0	−20	
	0	0	6	0	0	0	−20	
175	3	1	3	0	0	0	−5	
	1	3	3	0	0	0	−5	
	3	0	2	2	0	0	−14	
200	4	4	0	0	0	0	+11	
	4	0	0	4	0	0	−13	
	0	4	0	4	0	0	−14	
225	1	1	3	4	0	0	−5	
250	4	0	0	3	1	1	−8	
	1	1	2	2	0	2	−12	
275	2	1	2	4	0	1	−4	
	1	1	3	4	0	1	−5	
300	0	0	12	0	0	0	+56	

[a] f stands for the fcc hollow site, h stands for the hcp hollow site, b is a bridge site, t is the atop site, s is a subsurface adsorption site, and p is H_2 molecule in the second layer. [b] For 25% coverage, the subsurface H can sit in an octahedral site (under an fcc hollow site), in a tetrahedral site formed by three metal atoms from the first layer and one metal atom from the second layer (under an hcp hollow site), or in a tetrahedral site formed by one metal atom from the first layer and three metal atoms from the second layer (under the atop site).

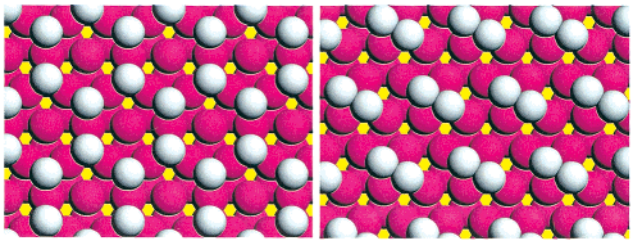

Figure 5. H adsorption at 50% coverage: 1H fcc + 1H hcp far (a) and close (b) adsorption (sharing one or two metal atoms on the surface).

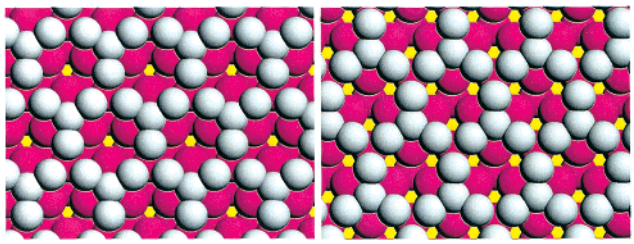

Figure 6. H adsorption at 100% coverage: 3H fcc + 1H hcp (a) and 1H fcc + 3H hcp (b).

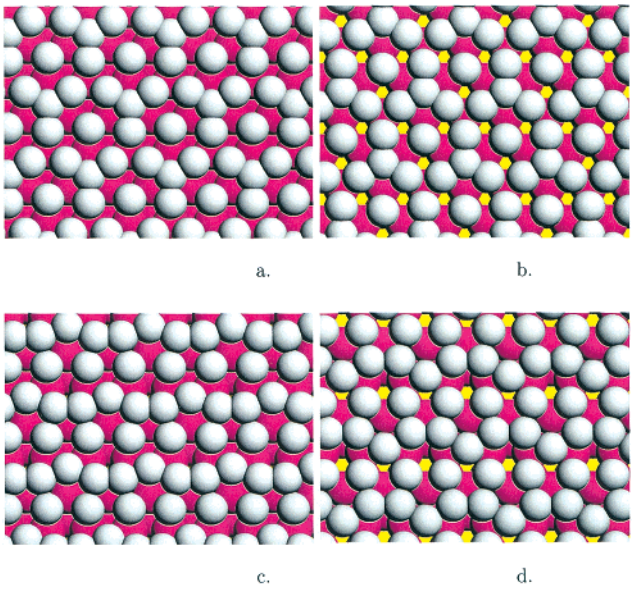

Figure 7. H adsorption at 125% coverage: 4H fcc + 1H hcp (a), 1H fcc + 4H hcp (b), 3H fcc + 2H bridge (c), and 3H hcp + 2H bridge (d).

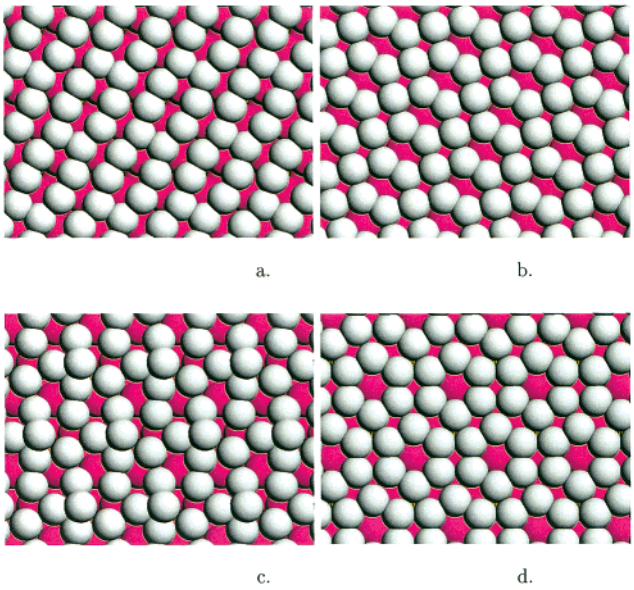

Figure 8. H adsorption at 150% coverage: 1H fcc + 1H hcp + 4H bridge (a), 2H fcc + 2H hcp + 2H bridge (b), 2H fcc + 1H hcp + 2H bridge + 1H atop (c), and 6H bridge (d).

and the Ru−H_{H_2} distance is 4.16 Å for one molecule and 4.32 and 4.60 Å for the other one.

The 275% coverage is also characterized by the presence of the second H layer, but this time, the H_2 molecules are

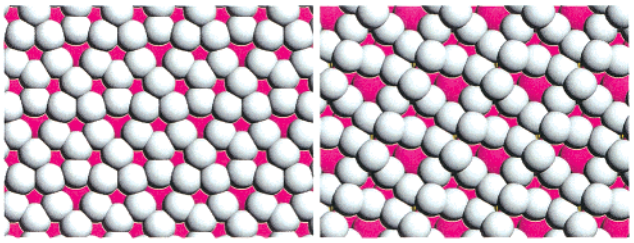

Figure 9. H adsorption at 175% coverage: 3H fcc + 1H hcp + 3H bridge (a) and 3H fcc + 2H bridge + 2H atop (b). The 1H fcc + 3H hcp + 3H bridge configuration is similar to that of the first case.

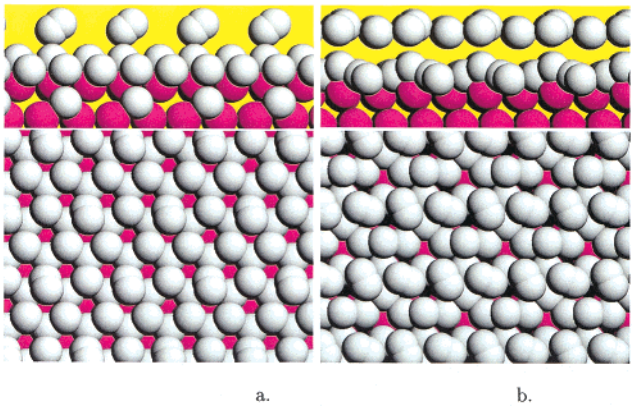

Figure 10. H adsorption at 250% coverage: 4H fcc + 3H atop + 1H subsurface + $1H_2$ (a) and 1H fcc + 2H hcp + H bridge + H atop + $2H_2$ (b). Top and side views.

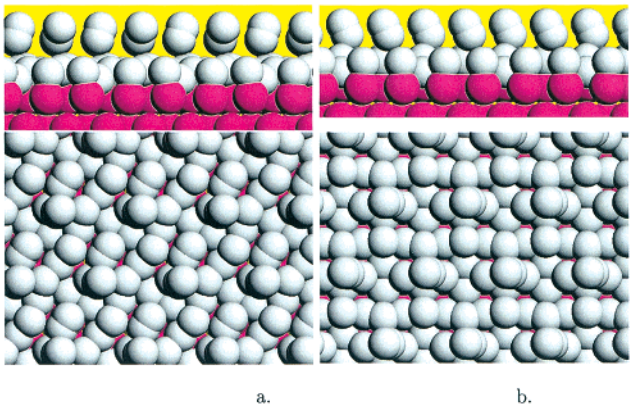

Figure 11. H adsorption at 275% coverage: 1H fcc + 1H atop + 2H bridge + 5H atop + $1H_2$ (a) and 2H fcc+ 1H hcp + 2H bridge + 4H atop + $1H_2$ (b). Top and side views.

perpendicular to the surface; see Figure 11. For the (a) structure, the H−H bond is 0.75 Å, and the Ru−H_{H_2} separation is 3.99 Å. The H_{H_2}−H_{atop} is 2.38 Å. There are five H atoms adsorbed atop on only four metal atoms! One Ru atom is shared by two H atoms, and the Ru−H bond length is 1.92 Å, longer than that for the other atop H atoms. The (b) structure is characterized by a Ru−H_{H_2} separation of 3.59 Å and a H_{H_2}−H_{atop} separation of 2.04 Å. The rest of the bonds are in the mentioned limits.

In the case of 300% coverage, 1 ML of H atoms, all adsorbed in bridge sites (all bridge sites occupied), is less stable than the H_2 in the gas phase with +56 kJ mol^{-1}!

As we can see from Figure 4, the adsorption energy of H atom does not change up to 100% coverage. This is due to the weak lateral interactions of the H atoms. Calculations for adsorbed H in $\sqrt{3} \times \sqrt{3}$ and 3×3 structures have been

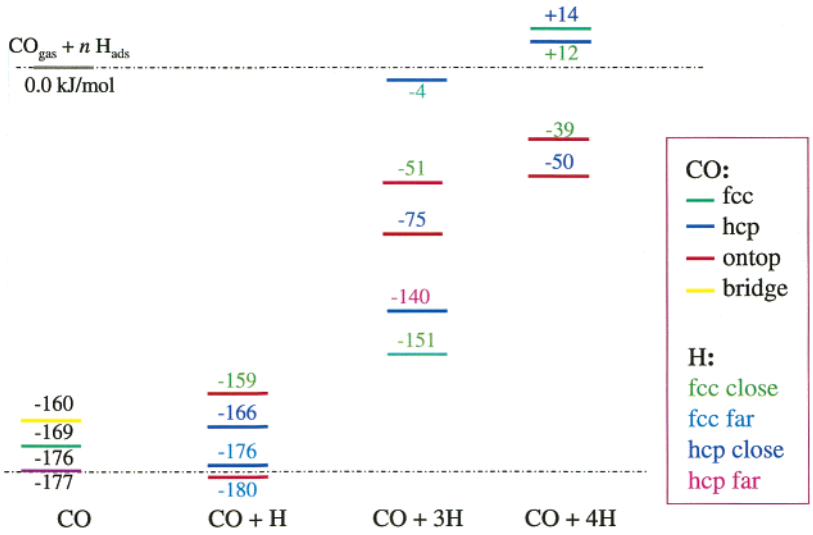

Figure 12. Energy diagram (in kJ mol^{-1}) with respect to H_2 and CO in the gas phase for H and CO coadsorption.

performed, but the adsorption energies and the geometry are similar to those of the 2 × 2 case.

For coverages up to 150%, H adsorption is still stable, so such configurations should be stable if the H layer is compressed. However, the dissociation of H_2 cannot lead to such structures because of the lack of empty sites for the dissociation reactions.

Up to 200% coverage, the adsorption energies are still less than zero but close to it. Those structures can be stable only at high pressures. For coverages up to 300%, we see a deviation of the linear increase if the adsorption energies are due to the formation of the second layer and to subsurface adsorption.

3.3. Hydrogen−Carbon Monoxide Coadsorption on the Ru(0001) Surface. Concerning the H coadsorption, we study in a 2 × 2 unit cell the interaction of one CO molecule with one, three, and four H atoms in several different adsorption sites, corresponding to a 25% coverage of CO and 25, 75, and 100% coverages of H, respectively. See Figure 12 for the adsorption energies.

For the interaction of CO with one H atom, we consider the cases when CO is adsorbed atop or hcp. For the atop adsorption of CO, the H atom was adsorbed in fcc sites close to CO (sharing one metal atom) or far away (without sharing metal atoms). The CO adsorption energy is −180 kJ mol for the far adsorption and −159 kJ mol^{-1} for the close adsorption. In this last case, the CO molecule is tilted.

For the CO adsorbed in the hcp site, we considered three adsorption sites similar to the CH_x and H coadsorption[41]—an hcp site (where H and CO share one metal atom on the surface), a close fcc site (where CO and H share two metal atoms), and a far fcc site (where CO and H share one metal atom and they are opposite). The adsorption energies are −176 kJ mol^{-1} for the far situation and −166 kJ mol^{-1} for the same type of site adsorption. The situation where the coadsorbed species were too close stabilize by the translation of CO to a near top site.

The coadsorption of a CO molecule with three H atoms gives a total coverage of 100%. For the CO adsorbed atop, four different adsorption sites were considered for H adsorption. The first one is with two H atoms in close fcc site (one metal atom shared on the surface) and one H atom in a far fcc site (no sharing of metal atoms on the surface). The second is when all three H atoms are in close fcc sites. The next two cases are similar to the first two ones, except that instead of fcc sites the H atoms are in hcp sites. The adsorption energies are −51 kJ mol^{-1} for CO atop and three H close fcc and −75 kJ mol^{-1} for CO atop and three H close hcp. The other two situations result in structures with CO adsorbed in the same site as the three H atoms.

For the CO-adsorbed hcp, the H atoms can adsorb in the other hcp sites. Another way is in fcc sites, two close and one far or three close. The adsorption energies are −140 kJ mol^{-1} for the hcp adsorption of the three H atoms and −4 kJ mol^{-1} for the close fcc adsorption. The case when two H atoms are in a close fcc site and one H is in a far fcc site leads to a migration of the CO molecule to the empty fcc site.

For the CO-adsorbed fcc, the H atoms were adsorbed on the other fcc site. The adsorption energy is −151 kJ mol^{-1}.

For the coadsorption of one CO molecule and four H atoms on a 2 × 2 unit cell, the total coverage is 125%. This may look strange, but evidence that the H monolayer on metal surfaces can be compressed exists, both from experiments[3] and from theory (see previous subsection). Four cases were considered: CO atop with four H atoms in fcc sites, CO atop with four H atoms in hcp sites, CO hcp with four H atoms in fcc sites, and CO fcc with four H atoms in hcp sites. The adsorption energy is −39×, −50×, +14×, and +12 kJ × mol^{-1}, respectively. The positive value means that CO is more stable in the gas phase; there is no adsorption. The C−O bond length is not changed by the H coadsorption. The C−Ru bond lengths are also not influenced by the coadsorption. The O−C−Ru and Ru−C−Ru angles are more affected but in general by less than 2−3°. The H atom is the most disturbed by the coadsorption with CO. The H−Ru bond lengths are little affected only at low coverage of H (25% CO + 25% H), whereas at higher coverage of H, the three bonds are no longer equivalent—one is getting shorter than 1.9 Å and the other two are longer than 2.1 Å. The Ru−H−Ru angles are also little affected at lower coverage (less than 5°) and more affected at higher H coverage (+6 to −19°). To analyze island formation, we calculated for the CO + 3H and CO + 4H systems the following parameters:

$$x = a - b - c - n*d/2$$

and

$$y = e - b - c + f - b - n*d/2$$

where

- a = energy of CO and nH on Ru(0001)
- b = energy of the Ru(0001) slab
- c = energy of CO gas
- d = energy of H_2 gas
- e = energy of CO on Ru(0001)
- f = energy of nH on Ru(0001)
- x = adsorption energy of CO and nH on Ru(0001)
- y = adsorption energy of CO on Ru(0001) + adsorption energy of nH on Ru(0001)

Here, n can be 3 or 4 (hydrogen atoms). Now, if $|x| < |y|$, we have island formation, and if $|x| > |y|$, we have *no* island formation. For all the 12 tests, the calculations described the situation before we found that island formation is favorable. The closest situation (11 kJ mol^{-1} difference between x and y) is for the CO fcc + 3H fcc system. These results, which indicate that H and CO prefer to make islands, support the conclusion of White et al.[17] that H and CO form segregated structures. The influence of entropy is not investigated since our calculations are performed at 0 K.

DOS diagrams (not shown)[13] for the CO and H coadsorption were also studied, and the ability of CO to adsorb strongly even on a fully covered surface with hydrogen was explained by the fact that the Ru atom where CO will bind is pushed upward and by doing that the electrons donated by the H atoms, which initially occupied the antibonding d-band regime, deplete this. Therefore, Ru is able to form a bond with CO at the cost of weakening its bonds with the other Ru atoms.

4. Conclusions

CO adsorbs strongly to the close-packed surface of ruthenium. At lower coverage, the atop site is preferred up to 25%. The lateral interaction of the CO adsorbed atop and CO adsorbed hcp is different, the hcp site having the smallest lateral interaction. The adsorption sites located near a step are more favorable, with about 20 kJ mol^{-1} for both atop and hcp sites and with about 10 kJ mol^{-1} for sites located at the bottom of the steps.

Local density of states plots are provided for a better understanding of the adsorption energy differences.

The lateral interactions of CO are repulsive above 33.3% coverage but are attractive at lower coverage such that the CO molecules prefers to form this structure ($\sqrt{3} \times \sqrt{3}$R30°) even at coverages lower than 33.3%.

Atomic hydrogen can form compressed layers on the Ru(0001) surface. Up to 100% coverage, the adsorption energy does not change. Up to 150% coverage, the lateral interaction is still acceptable. After 200% coverage, the adsorption energy goes to zero and the second layer of hydrogen atoms is built.

For the H coadsorption with CO, the lateral interactions are repulsive, and H and CO prefer to segregate rather than to form mixed structures.

At low coverages of H and CO, both species can adsorb on the preferred site (CO, atop; H, fcc). However, by increasing the H coverage, the H is forced to populate sites closer to CO molecule, and this leads to distortions of the H adsorption site (H−Ru bonds with different lengths). CO is little affected by the H coadsorption unless H is present at 100% coverage, when the CO will still adsorb on the atop sites with an important decrease of the adsorption energy.

Acknowledgment. This work is part of the research program of the Stichting voor Fundamenteel Onderzoek der Materie (FOM), which is financially supported by the Nederlandse organisatie voor Wetenschappelijk Onderzoek (NWO). This work has been accomplished under the auspices of NIOK, The Netherlands Institute for Catalysis Research, Lab Report No. TUE-2001-5-4. The calculations have been partially performed with NCF support (SC183, SC521, MP43a). Authors thank Professor Hafner for the vasp code and Dr. Eric Meijer for his help in computing the CO frequencies.

References and Notes

(1) Toyoshima, I.; Somorjai, G. A. *Catal. Rev.—Sci. Eng.* **1997**, *19*, 105.
(2) Storch, H. N.; Golumbic, N.; Anderson, R. B. *The Fischer−Tropsch and Related Syntheses, Including a Summary of Theoretical and Applied Contact Catalysis*; Wiley: New York, 1951.
(3) Sun, Y. K.; Weinberg, W. H. *Surf. Sci.* **1989**, *214*, L246.
(4) Shi, H.; Jacobi, K. *Surf. Sci.* **1994**, *313*, 289.
(5) Fuggle, J. C.; Madey, T. E.; Steinkilberg, M.; Menzel, D. *Surf. Sci.* **1975**, *52*, 521.
(6) Pfnuir, H.; Menzel, D.; Hoffmann, F. M.; Ortega, A.; Bradshaw, A. M. *Surf. Sci.* **1980**, *93*, 431.
(7) Fuggle, J. C.; Madey, T. E.; Steinkilberg, M.; Menzel, D. *Chem. Phys.* **1975**, *11*, 307.
(8) Pfnuir, H.; Menzel, D. *J. Chem. Phys.* **1983**, *79*, 2400.
(9) Pfnuir, H.; Feulner, P.; Menzel, D. *Chem. Phys. Lett.* **1979**, *59*, 481.
(10) Pfnuir, H.; Feulner, P.; Menzel, D. *J. Chem. Phys.* **1983**, *79*, 4613.
(11) Berenbak, B.; Butler, D. A.; Riedmller, B.; Papageorgopoulos, D. C.; Stolte, S.; Kleyn, A. W. *Surf. Sci.* **1998**, *414*, 271.
(12) Riedmiller, B.; Ciobica, I. M.; Papageorgopoulos, D. C.; Berenbak, B.; van Santen, R. A.; Kleyn, A. W. *Surf. Sci.* **2000**, *465*, 347.
(13) Riedmiller, B.; Ciobica, I. M.; Papageorgopoulos, F.; Berenbak, B.; van Santen, R. A.; Kleyn, A. W. *J. Chem. Phys.* **2001**, *115*, 5244.
(14) Berenbak, B.; Riedmiller, B.; Rettner, C. T.; Auerbach, D. J.; Stolte, S.; Kleyn, A. W. *PhysChemComm* **2001**, *16*, 1.
(15) Butler, D. A.; Berenbak, B.; Stolte, S.; Kleyn, A. W. *Phys. Rev. Lett.* **1997**, *78*, 4653.
(16) Berenbak, B.; Riedmller, B.; Butler, D. A.; Rettner, C. T.; Auerbach, D. J.; Stolte, S.; Kleyn, A. W. *Phys. Chem. Chem. Phys.* **2000**, *2*, 919−923.
(17) White, J. M.; Akhter, S. *CRC Crit. Rev. Solid State Mater. Sci.* **1988**, *14*, 130.
(18) Riedmller, B.; Papageorgopoulos, D. C.; Berenbak, B.; van Santen, R. A.; Kleyn, A. W. To be submitted for publication.
(19) Delbecq, F.; Moraweck, B.; Vérité, L. *Surf. Sci.* **1998**, 396.
(20) Delbecq, F.; Sautet, P. *Chem. Phys. Lett.* **1999**, *302*, 91.
(21) Delbecq, F.; Sautet, P. *Phys. Rev. B* **1999**, *59*, 5142.
(22) Eichler, A.; Hafner, J. *J. Chem. Phys.* **1998**, *109*, 5585.
(23) Hammer, B.; Nielsen, O. H.; Nørskov, J. K. *Catal. Lett.* **1997**, *46*, 31.
(24) Curulla, D.; Clotet, A.; Ricart, J. M. *J. Phys. Chem. B* **1999**, *103*, 5246.
(25) Hammer, B.; Morikawa, Y.; Nørskov, J. K. *Phys. Rev. Lett.* **1996**, *76*, 2141.
(26) Wang, R. L. C; Kreuzer, H. J.; Menzel, D. *Z. Phys. Chem.* **1997**, *202*, 205.
(27) Peebles, D. E.; Schreifels, J. A.; White, J. M. *Surf. Sci.* **1982**, *116*, 117.
(28) Mak, C. H.; Deckert, A. A.; George, S. M. *J. Chem. Phys. 8*, 5242 (89).
(29) Kresse, G.; Furthmüller, J. *Comput. Mater. Sci.* **1996**, *6*, 5.
(30) Kresse, G.; Furthmüller, J. *Phys. Rev. B* **1996**, *54*, 96.
(31) Perdew, J. P. *Electronic Structure of Solids '91*; Akademie Verlag: Berlin, 1991.
(32) Methfessel, M.; Paxton, A. T. *Phys. Rev. B* **1989**, *40*, 3616.
(33) Vanderbilt, D. *Phys. Rev. B* **1990**, *41*, 7892.
(34) Kresse, G.; Hafner, J. *J. Phys.: Condens. Matter* **1994**, *6*, 8245.
(35) Ciobica, I. M.; Frechard, F.; van Santen, R. A.; Kleyn, A. W.; Hafner, J. *Chem. Phys. Lett.* **1999**, *311*, 185.
(36) Lahaye, R. J. W. E.; Stolte, S.; Holloway, S.; Kleyn, A. W. *J. Chem. Phys.* **1996**, *104*, 8301.
(37) Meijer, E. L. Quantum Chemical Computation of Infrared Spectra of Acidic Zeolites. Ph.D. Thesis, Eindhoven University of Technology, Eindhoven, The Netherlands, September 2000.
(38) Jacob, P. *Phys. Rev. Lett.* **1996**, *77*, 4229.
(39) Jachimowski, T. A.; Meng, B.; Johnson, D. F.; Weinberg, W. H. *J. Vac. Sci. Technol., A* **1995**, *13*, 1564.
(40) Jacob, P.; Person, B. N. J. *Phys. Rev. Lett.* **1997**, *78*, 3503.
(41) Ciobica, I. M.; Frechard, F.; van Santen, R. A.; Kleyn, A. W.; Hafner, J. *J. Phys. Chem. B* **2000**, *104*, 3364.